DNA methylation of ICAM4 and NOXO1 participate in the formation of uterine fibroids via regulating immune cell infiltration

Yafei Zhu[#], Wei Shi[#], Wenling Han, Maohuai Wang, Jie Chen, Jieli Zhou[*]

Department of Gynecology, the First Affiliated Hospital of Gannan Medical University,128 Jinling Road, Zhanggong District, Ganzhou City, Jiangxi 341000, China

[#]contributed equally to this work

ARTICLE INFO	ABSTRACT
	This atudy aimed to reveal the effect of DNA methylation on immune infiltration of uterine fibroids (UFs) and to further classify UFs based on transcriptomic characteristics. The transcriptome and DNA methylation data of UFs were collected from the GEO database. After taking the intersection of the differentially expressed genes in these two types of data, the intersection gene was used to draw ROC curves and to filtrate the candidate genes with AUC≥0.8. Immune infiltration analysis was performed in the online tool EPIC. The correlation between gene with AUC≥0.8 and the abundance of each immune cell type was calculated with |R|>0.3 and P<0.05. ConsensusClusterPlus package in R software was used to further cluster the samples of UFs. In this study, a total of 41 RNA-seq data (10 normal uterine samples and 31 UFs samples) and 34 DNA methylation data (10 from normal subjects and 24 from patients with UFs) were involved. The significantly down-regulated ICAM4, SPECC1L, and NOXO1 were the top three methylated drive genes of UFs. Therefore, NOXO1 and ICAM4 present an intimate correlation to immune cell infiltration. Besides, UFs could be clustered into two subtypes, including a TSAB1 up-regulated subtype and a FOSB up-regulated subtype. DNA methylation of ICAM4 and NOXO1 are involved in the pathogenesis of UFs via regulating immune cell infiltration. Further classification based on transcriptomic characteristics could divide UFs into sexual steroids-related and biomechanics-related subtypes, which would promote its non-invasive treatment.

Introduction

Uterine fibroids are the most common tumors in women, accounting for approximately 52% of the benign tumors of the female reproductive system, and the prevalence rate is as high as 60% in child-bearing age women and more than 70% in women after menopause (1-3). It is produced by muscular stem cells altered by a single gene alteration under the influence of gonadal hormones and developed in the muscle layer of the smooth muscle tissue of the uterus with single or multiple lesions and varying size (4,5). The symptoms of uterine fibroids usually manifest as abnormal uterine bleeding, pelvic hypertrophy, and ultimate infertility (6-8). Therefore, uterine fibroids have a serious negative impact on society and the life quality of women (9).

Although pharmaceutical therapies and minimally invasive surgery are widely adopted to deal with uterine fibroids, these therapies are not curative (10). Currently, approximately 30-40% of performed hysterectomies are caused by uterine fibroid (10,11). As time progresses, increasing advances have been made in order to explore less invasive techniques as well as non-surgical treatments to cure uterine fibroids (11).

With the development of high-throughput sequencing technology, transcriptome sequencing (RNA-seq) is increasingly used in the life sciences to study gene-gene as well as gene-symptom relationships (12,13). Since RNA-seq opens new avenues for exploring effective treatment for uterine fibroids, Li et al. (14) found that transcription factor XBP1 can regulate ITGA2, affect the downstream PI3K/AKT signaling pathway, and eventually adjust the proliferation of uterine fibroids. Carbajo-García et al. (15) found that the instability of H3K4me3 changes the expression level of oncogenes as well as tumor suppressor genes, and finally induces the aberrant proliferation of uterine fibroids, in which dysregulated Wnt/β-catenin, and TGF-β pathways are participated. Besides, Carbajo-García et al. (16) also revealed that the acetylation of H3K27 regulates the expression of genes involved in proliferation, cell signaling, cell transport, angiogenesis and extracellular matrix formation of uterine fibroids. Since the entire number of participants of uterine fibroids has not been revealed, an extensive study based on a larger sample size was of urgent need.

Virtually, all cells in an organism contain the same genetic information, however, not all genes are expressed simultaneously by all cell types (17). Methylation, an important type of epigenetic regulation that mediates the diversified gene expression, refers to the transfer of active methyl groups to the target location catalyzed by methyltransferase without altering DNA sequence composition (17). Recent technical developments have made it possible to perform genome-wide DNA methylation analysis. For

---

* Corresponding author. Email: zhuyafeizyf@outlook.com

example, Li et al (18). previously revealed that aberrant methylation of the E-cadherin gene may participate in the formation of uterine fibroids.

However, the combined application of RNA-seq and DNA methylation in the uterine fibroids field has not been studied, which could provide a series of latent pathogenic mechanisms. As a result, we collected all public RNA-seq and DNA methylation data from public databases and performed pooled analysis to reveal the mechanism of DNA methylation in uterine fibroids. Besides, just as with other tumors, immune infiltration plays a significant role in the occurrence and development process (2). Thus, this study mainly focused on the effect of DNA methylation on immune infiltration of uterine fibroids.

Materials and Methods

RNA-seq data collection and analysis

Using the keyword "uterine fibroids", we collected the GSE199849 transcriptome data from the GEO database (https://www.ncbi.nlm.nih.gov/geo). A total of 10 normal uterine samples and 31 samples from uterine fibroids were involved in this study. The reads count was collected to generate the expression matrix. The SVA package of R software (v4.2.2) was used for batch correction of RNA-seq data. Deseq2 software (https://github.com/mike-love/DESeq2) was used to conduct differential expression analysis according to the expression levels of the control group and the patient group, based on padj<0.05, log2FoldChange>1 or log2FoldChange<-1. The pheatmap package of R software was used to draw the heatmap according to the normalized data, and the ggplot2 package was used to draw the volcano plot according to the P value and foldchange value in the differential expression analysis results.

Methylation data collection and analysis

Methylation data of uterine fibroids, based on the keyword "uterine fibroids", was extracted from GSE120854 in the GEO database. A total of 34 samples of myometrium were collected, including 10 normal subjects and 24 patients with uterine fibroids. Differential methylation analyses were implemented in DMRcate software, with the parameters being P<0.05 and absolute beta-value > 0.2. Then, the results of differential methylation analysis between the control group and the patient group were obtained.

Driver gene identification

We extracted the intersection genes of the differential genes in transcriptome and methylation results and used the sklearn module of Python to draw the receiver operating characteristic (ROC) curve for each intersection gene based on their respective expression levels. Genes with an area under curve (AUC) greater than 0.8 were selected as the driving genes for this uterine fibroid data. Based on the expression of the drive gene, the ConsensusClusterPlus package in R software was used to further cluster to obtain subgroups of uterine fibroids patients. The Prcomp package in R software was used for drawing PCA plots in order to visualize the clustered samples.

Analysis of mutation among clusters

Fastp software was used to conduct quality control for the fastq data from the GEO database, and the sequence with low quality was removed to obtain clean data. STAR software was used to map clean data to the hg19 genome. Samtools and varscan2 software were used for mutation identification. VEP was used for the functional annotation of mutations. The Maftools module of R software was used for summarizing and mapping mutations in each sample.

Analysis of differentially expressed genes among clusters

For each cluster, deseq2 was used for pairwise differential expression analysis with the analysis parameter being padj<0.05, log2FoldChange>1 or log2FoldChange<-1. The difference expression between the two clusters was obtained. Then, the pheatmap package of R software was used to draw heat maps based on the normalized data, and the ggplot2 package was used to draw a volcano plot according to the results of the difference analysis of the P value and foldchange value.

Immune infiltration analysis

We use online analysis tools EPIC (https://gfellerlab.shinyapps.io/EPIC_1-1/) based on the gene expression of each sample to analyze immune infiltration. Then, the result of samples related to immune infiltrate abundance was obtained. Cor.test function of R software was used to calculate the Spearman correlation of each cell and drive genes (P<0.05 means significant correlation).

Analysis of genes related to ferroptosis

A list from http://www.zhounan.org/ferrdb/current/ was collected to generate ferroptosis-related genes. After mapping to drive genes to obtain intersection genes, the obtained genes can be considered as ferroptosis-related driver genes.

WGCNA analysis

Based on the gene expression of each cluster, co-expression analysis was carried out using the WGNCA package of R software, with default parameters. After selecting key modules, a clusterprofiler package was used for GO analysis.

Results

Differentially expressed genes and methylated genes in uterine fibroids

According to the gene expression matrix of the control group and uterine fibroids group in the GSE199849 dataset, 564 differentially expressed genes were obtained, of which 62 were up-regulated and 502 were down-regulated. (Figure 1)

Based on the GSE120854 dataset, we obtained 13,364 differential methylation probes belonging to 5623 genes. Among them, 8646 probes were hypermethylated and 4718 were hypomethylated (Figure 2). The top 20 genes with the largest number of differential methylation probes were presented in Figure 2C.

Potential methylated driver genes of uterine fibroids

The differentially expressed genes and differentially methylated genes in uterine fibroids were intersected to obtain the 155 intersection genes. (Figure 3A) After the intersecting, ROC curves were drawn for each intersection genes according to the expression level and group rela-
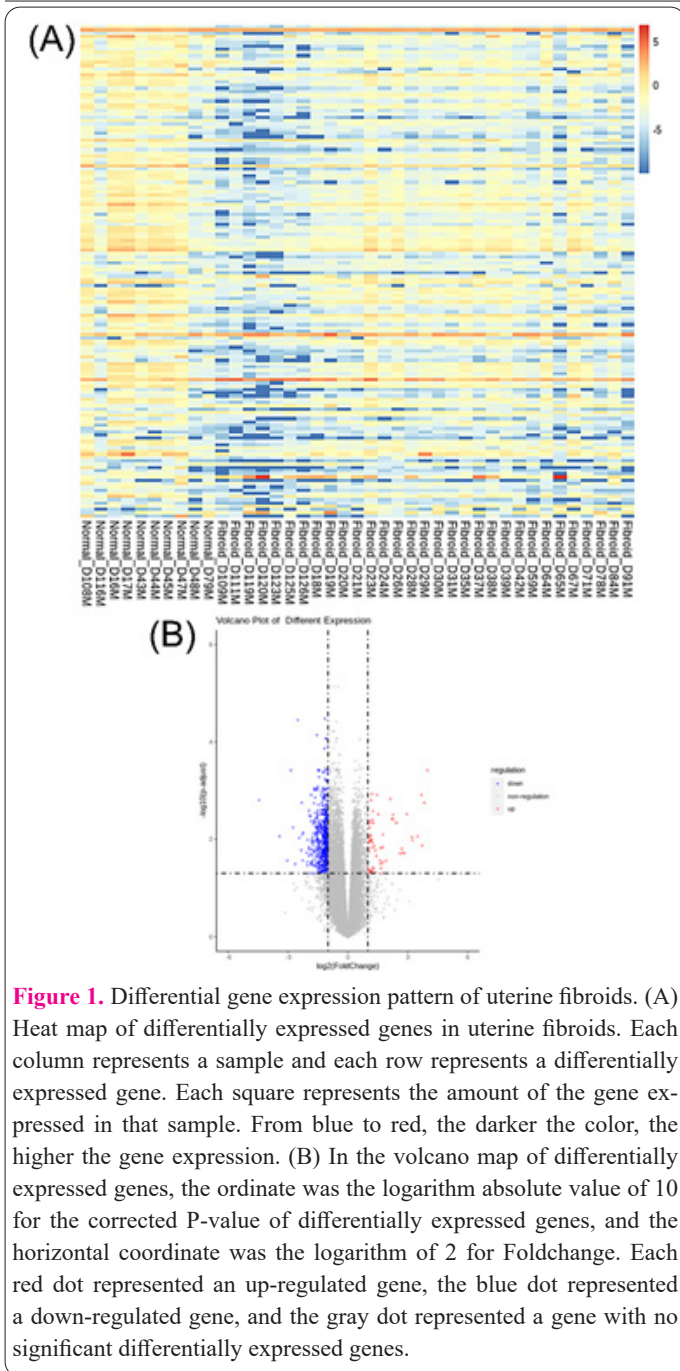
Figure 1. Differential gene expression pattern of uterine fibroids. (A) Heat map of differentially expressed genes in uterine fibroids. Each column represents a sample and each row represents a differentially expressed gene. Each square represents the amount of the gene expressed in that sample. From blue to red, the darker the color, the higher the gene expression. (B) In the volcano map of differentially expressed genes, the ordinate was the logarithm absolute value of 10 for the corrected P-value of differentially expressed genes, and the horizontal coordinate was the logarithm of 2 for Foldchange. Each red dot represented an up-regulated gene, the blue dot represented a down-regulated gene, and the gray dot represented a gene with no significant differentially expressed genes.

Figure 2. Differential gene methylation pattern of uterine fibroids. (A) Heat map of gene methylation pattern in uterine fibroids. (B) The volcano map of differential gene methylation pattern in uterine fibroids. (C) The top 20 genes with the largest number of differential methylation probes.

Figure 3. Potential methylated driver genes of uterine fibroids. (A) Venn diagram of differentially expressed genes and differentially methylated genes in uterine fibroids. (B) A total of 36 genes with AUC≥0.8 according to the expression level and group relationship were selected as driver genes. (C) ROC curves of the top three driver genes with the highest AUC. The ordinate is the true positive rate and the abscissa is the false positive rate. The larger the AUC area, the higher the accuracy for using the gene to distinguish the two subtypes of uterine fibroids. (D) The heatmap of gene expression levels of 36 driver genes for uterine fibroids sample. (E) PCA plot of 36 driver genes for uterine fibroids sample. Different colors represent different clusters of samples.

tionship, and a total of 36 genes with AUC≥0.8 were selected as driver genes (Figure 3B). The top three driver genes with the highest AUC were shown in Figure 3C. That is, the methylation of ICAM4 (RNA-seq: log2FoldChange= -1.0426; padj= 0.0012), SPECC1L (RNA-seq: log2FoldChange= -1.8487; padj= 0.0042), and NOXO1 (RNA-seq: log2FoldChange= -1.6454; padj= 0.0014) could be deemed as the important participant in the pathogenetic process of uterine fibroids.

According to the expression levels of 36 driver genes, a heatmap with clustering was drawn to preliminarily differentiate all samples of uterine fibroids (Figure 3D). The uterine fibroids can be divided into two clusters according to the clustering situation. Further PCA analysis also verify these two cluster (Figure 3E).

The difference of gene mutation for the two clusters of uterine fibroids

Single nucleotide mutation, insertion mutation and deletion mutation were analyzed for each sample. The genes with significa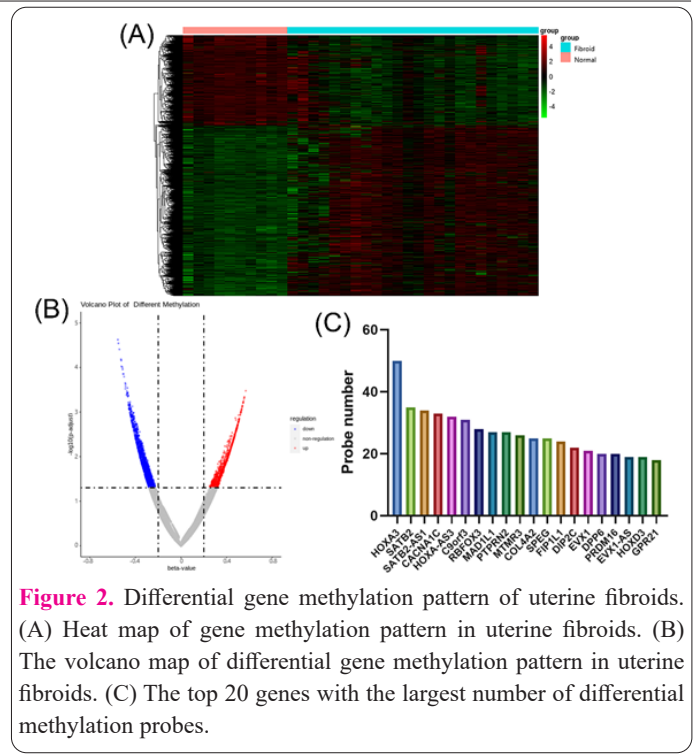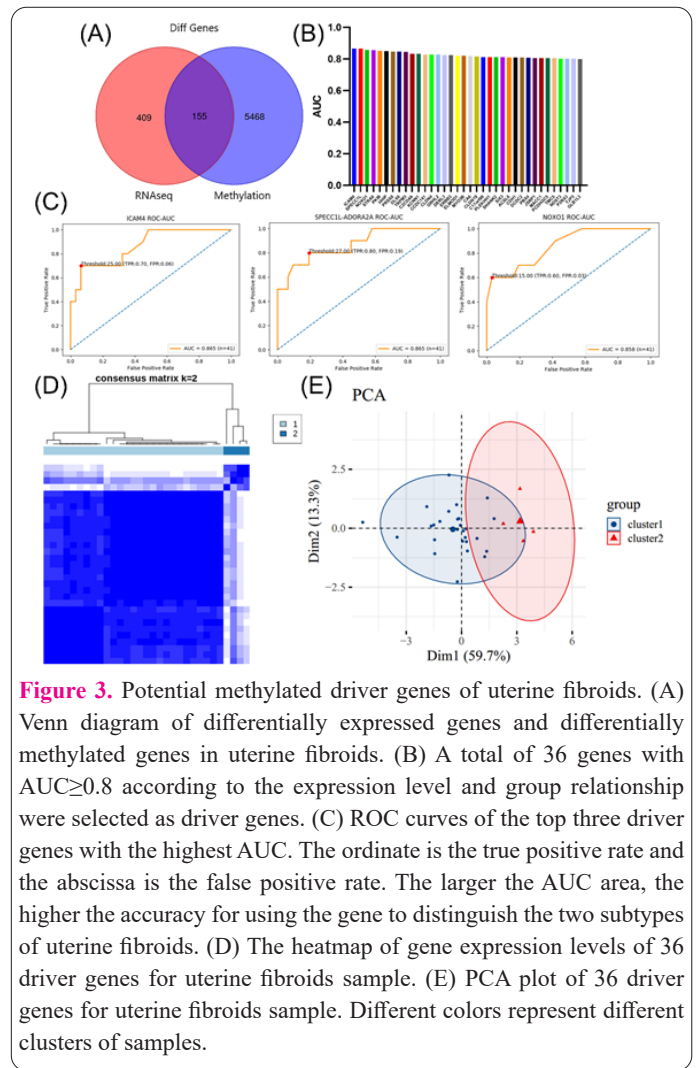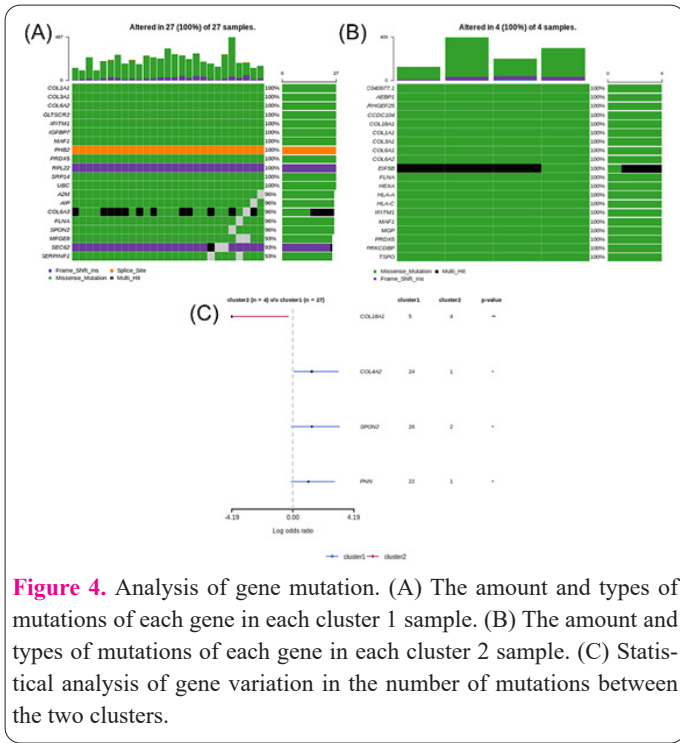nt differences in mutation between clusters were counted and presented in Figure 4. Thereinto, splice-site mutations of prohibitin 2 (PHB2) and frameshift insert mutation of RPL22 (a ribosomal protein component of the large 60S subunit) were conservative mutations in cluster1. On the other hand, a multi-hit mutation of EIF5B (a eukaryotic translation initiation factor) was usually detec-

Figure 4. Analysis of gene mutation. (A) The amount and types of mutations of each gene in each cluster 1 sample. (B) The amount and types of mutations of each gene in each cluster 2 sample. (C) Statistical analysis of gene variation in the number of mutations between the two clusters.

ted in cluster 2.

Differential gene expression of the two uterine fibroids clusters

After conducting further differential gene expression analysis of the 31 uterine fibroids samples, we obtained two clusters and a total of 17 significantly differentially expressed genes. Compared with cluster 1, cluster 2 presented down-regulated TPSAB1, CARTPT, CXCL13, ESYT3, CPA4, CDC7, and PENK and up-regulated SLC35F1, RGS9, KLF2, EGR1, FOS, IER2, FOSB, PPP1R15A, JUN, and ZFP36 (Figure 5A-B). No driver gene (AUC≥0.8) was found in differentially expressed genes.

After mapping the differentially expressed gene to familiar cell fate, we found that ferroptosis-related NRG3 and TP63 were significantly down-regulated in uterine fibroid (Figure 5C). However, when compared with cluster 1, cluster 2 of uterine fibroid presented up-regulated ferroptosis related KLF2, JUN, EGR1, and ZFP36 (Figure 5D).

Differential immune cell infiltration pattern of the two uterine fibroids subtype

There is a great relationship between immune infiltration and prognosis. We used the EPIC tool to analyze the gene expression data of each sample to obtain the abundance of immune cells of each sample. Then, according to the expression levels of 152 driver genes, the correlation between each gene and the abundance of each cell species was calculated. A total of 149 driver genes were significantly correlated with immune infiltration. The cell type differences between clusters were analyzed using the student T-test with $P < 0.05$.

Uterine fibroids are mainly infiltrated by CAFs, CD4+ T cells, CD8+ T cells, and endothelial cells (Figure 6B). Among various immune cells, B cells and macrophages presented significant differences for the two uterine fibroids subtype (Figure 6C). According to |R|>0.3 and p<0.05, we found NOXO1 and ICAM4 present intimate correlation to
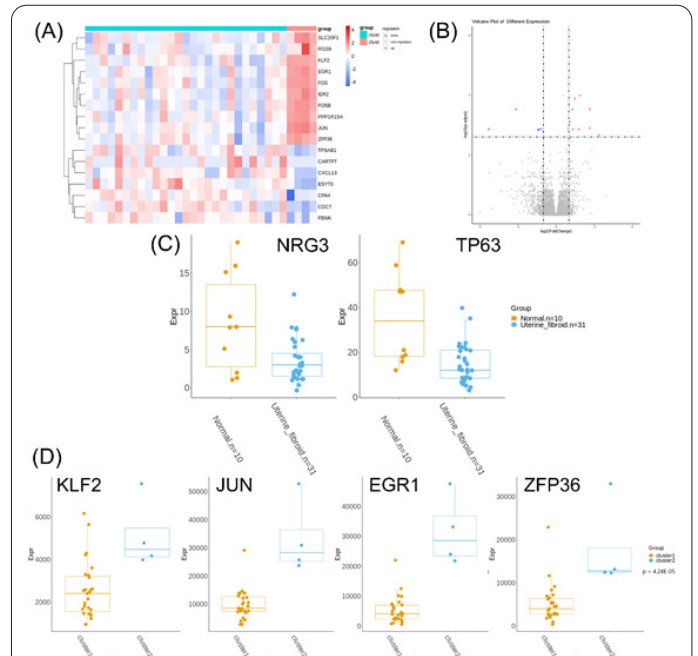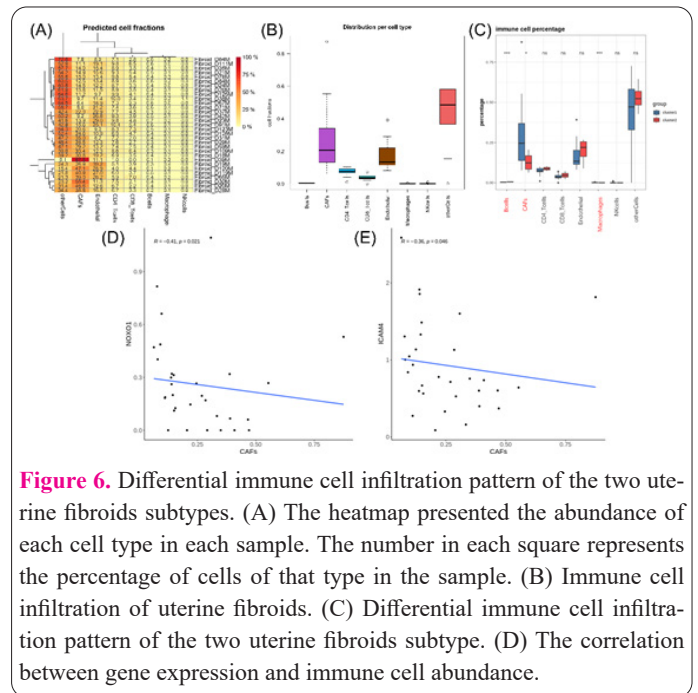

Figure 5. Differential gene expression of the two uterine fibroids subtypes. (A) Heat map of differential genes between clusters. (B) Volcano plot of clusters of differentially expressed genes. (C) Ferroptosis-related gene in normal uterus and uterine fibroid. (D) Differential expression of ferroptosis-related genes in the two uterine fibroids subtype.

Figure 6. Differential immune cell infiltration pattern of the two uterine fibroids subtypes. (A) The heatmap presented the abundance of each cell type in each sample. The number in each square represents the percentage of cells of that type in the sample. (B) Immune cell infiltration of uterine fibroids. (C) Differential immune cell infiltration pattern of the two uterine fibroids subtype. (D) The correlation between gene expression and immune cell abundance.

immune cell infiltration (Figure 6D-E). It's worth noting that NOXO1 and ICAM4 were potential drive genes in the pathogenetic process of uterine fibroids.

WGCNA analysis

According to gene expression levels between clusters, WCGNA software was used for co-expression analysis to obtain co-expression networks and genes in each module (Figure 7). A total of 16 modules were obtained, and cluster diagrams of these modules were also generated (Figure 7B). According to R and P values, genes in top three relevant modules (blue_M11 with cor=0.095 and p=0.016, orange_M15 with cor=0.45 and p=0.0052, and black_M6 with cor=0.35 and pxiaoyu) were selected for
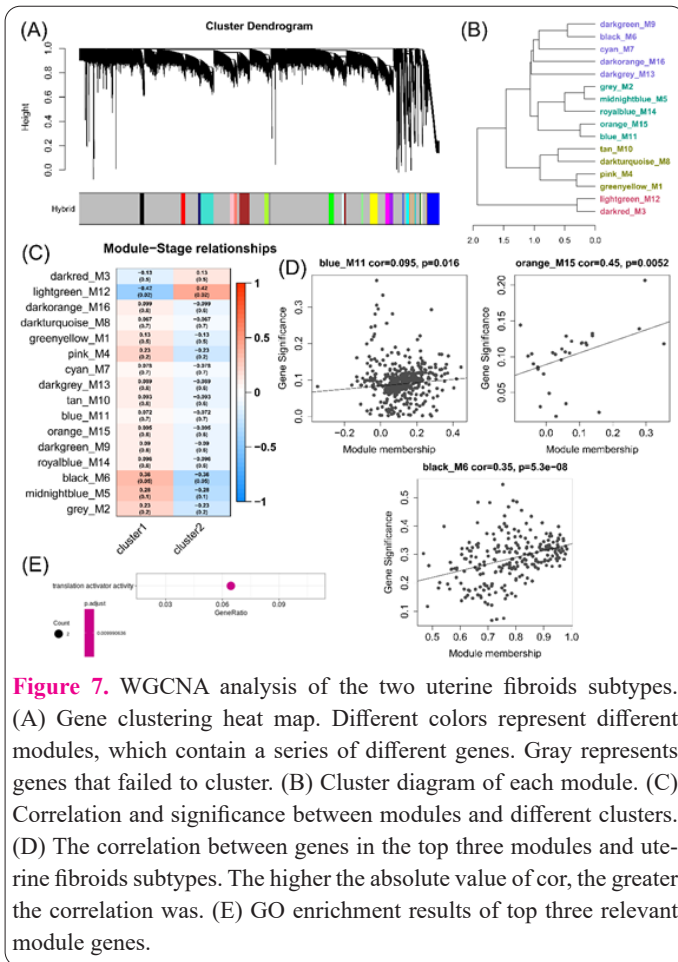
Figure 7. WGCNA analysis of the two uterine fibroids subtypes. (A) Gene clustering heat map. Different colors represent different modules, which contain a series of different genes. Gray represents genes that failed to cluster. (B) Cluster diagram of each module. (C) Correlation and significance between modules and different clusters. (D) The correlation between genes in the top three modules and uterine fibroids subtypes. The higher the absolute value of cor, the greater the correlation was. (E) GO enrichment results of top three relevant module genes.

GO pathway analysis. The results suggested that cluster 1 presented higher gene expression of translation activator activity than cluster 2 (Figure 7E).

Discussion

DNA methylation of ICAM4 and NOXO1 are involved in the pathogenesis of uterine fibroids via regulating immune cell infiltration

Over the past years, comprehensive sequencing of human cancer has revealed the landscapes of genomic characteristics of cancer (19). This landscape is composed of a series of frequently and infrequently altered genes (19,20). Thereinto, 140 genes were revealed as the drive genes in the tumorigenesis (20). Generally, a cancer involves two to eight driver gene mutations (20). Driver genes can be differentiated into three core functions of cellular processes: genome maintenance, cell survival, and cell fate (20).

In this study, we made a thorough data search in the public database to collect RNA-seq and DNA methylation data of uterine fibroids. A total of 41 RNA-seq were included in this study, including 10 normal uterine samples and 31 uterine fibroids samples. Besides, a total of 34 DNA methylation data of myometrium were collected, including 10 from normal subjects and 24 from patients with uterine fibroids. After taking the intersection of the differentially expressed genes in these two types of data and filtrating the candidate genes with AUC≥0.8, significantly down-regulated ICAM4, SPECC1L, and NOXO1 were the top three methylated drive genes of uterine fibroids.

Then, according to the expression levels of all 155 driver genes from RNA-seq data, the correlation between each gene and the abundance of each cell species was calculated. A total of 149 driver genes were significantly correlated with immune infiltration. According to |R|>0.3 and p<0.05, we found NOXO1 and ICAM4 present an intimate correlation to immune cell infiltration. Coincidentally, NOXO1 and ICAM4 were the top methylated drive genes of uterine fibroids. That is, DNA methylation of ICAM4 and NOXO1 are involved in the pathogenesis of uterine fibroids via regulating immune cell infiltration.

Kwangwoo et al. (21) previously found that variation in the ICAM4 locus is associated with the susceptibility of systemic lupus erythematosus, an autoimmune disease, in multiple ancestries. This finding just verified the correlation between ICAM4 and immune cell infiltration. In addition, NOXO1 was previously reported to participate in the tumorigenesis of colon cancer (22) and gastric cancer (23).

Classification of uterine fibroids based on transcriptomic characteristics would promote its non-invasive treatment

According to the different locations of the fibroids, the traditional classification method divides uterine fibroids into three types, namely, intramural myomas, subserous fibroids, and submucosal fibroids (24). With the development of minimally invasive technologies, the International Federation of Gynecology and Obstetrics (FIGO) classification system further divided uterine fibroids into types 0-8 based on the anatomical location, which can significantly improve the accuracy of clinical diagnosis and minimally invasive treatment (8). However, with the development of non-invasive treatment, targeted therapy could specifically resist uterine fibroid cells to eliminate tumor lesions with as little as possible insult to surrounding tissues, systemic hormones and fertility (25). Thus, further classification of uterine fibroids based on transcriptomic characteristics would promote its non-invasive treatment. In this study, it's worth noting that the 31 uterine fibroids samples could be clustered into two subtypes according to a total of 17 significantly differentially expressed genes, including 7 down-regulated genes and 10 up-regulated genes.

Mast cells abound in all layers of the human endometrium and play a vital role in extracellular matrix remodeling and angiogenesis (26). Mast cells from humans, mice, and rat can express estradiol and progesterone receptors, and female hormones can activate mast cells (27). Therefore, sexual steroids, in a dose-dependent manner, contribute to the maturation of mast cells and directly induce degranulation (27,28). Activated mast cells liberate a series of factors that attract other inflammatory cells and lead to collateral damage to surrounding tissues, which leads to scar formation and fibrosis (29). Among the 17 significantly differentially expressed genes in the two uterine fibroids clusters, TSAB1, the mast cells specific marker, was significantly up-regulated in cluster 1. That is, cluster 1 could be deemed as a sexual steroids-related uterine fibroids subtype. Besides, Krüppel-like factor 2 (KLF2), which belongs to a family of zinc finger-containing transcription factors and generally acts as an inhibitor of cell proliferation, was down-regulated in clusters 1 (26).

Since early growth response gene-1 (EGR1) was mainly reported to be significantly down-regulated in uterine fibroids, cluster 2 seems to be an unusual subtype. It's worth noting that FOSB was significantly up-regulated in cluster 2, which is consistent with the study made by Pilgrim et al. (30) FOSB was related to mechanical

stretch, for example, Ramachandran et al. (31) found that, when suffering mechanical stretch, FOSB in the bladder smooth muscle would up-regulate and cause the expression of ECM proteins up-regulate. Recently, Mitchell et al. (32) revealed that static stretch in rat myometrial smooth muscle can lead to increased expression of FOSB. After induced by stretch or stress, up-regulated FOSB could participate in the mechano-transduction of uterine fibroids (31). This mechano-transduction may facilitate fibrosis, cause enhancive collagen 1A deposition, and attenuated fibronectin deposition. These alterations in the extracellular matrix conduce to the dysregulation of collagen deposition, the stiffness of tissue, and the local microenvironment of the uterine fibroid. In addition, since Jin et al. previously found that mechano-transduction can promote ferroptosis in vascular smooth muscle cells, the difference in ferroptosis-related gene expression for the two clusters was consistent with the aforementioned deduction. That is, cluster 2 could be deemed as a biomechanics-related uterine fibroids subtype. Besides, since FOSB expression could be attenuated by macrophages (30), the significantly down-regulated macrophages infiltration pattern in cluster 2 was met expectation.

In conclusion, we have demonstrated that DNA methylation of ICAM4 and NOXO1 are involved in the pathogenesis of uterine fibroids via regulating immune cell infiltration. Besides, further classification based on transcriptomic characteristics could divide uterine fibroids into sexual steroids-related and biomechanics-related subtypes, which would promote its non-invasive treatment.

Funding

Conflict of Interests
The authors declared no conflict of interest.

References

1. Sefah N, Ndebele S, Prince L, et al. Uterine fibroids - Causes, impact, treatment, and lens to the African perspective. Front Pharmacol 2022; 13: 1045783.
2. Xu H, Wang G, Li Q, Zhang L, Zhang Y, Wu Y. Clinical Features, Management and Maternal-Infant Prognosis in Patients with Complete Uterine Rupture in the Second and Third Trimester of Pregnancy. Altern Ther Health M 2022; 28(6): 82-87.
3. Guan L, Xue L, Chu J, Xue J, Zhang S, Zhu L. Effect of Tiaojingzhixue Fang on the expression of sex hormone and endometrial tissue mRNA in perimenopausal patients with abnormal uterine bleeding. Cell Mol Biol 2021; 67(5): 317-323.
4. Aninye IO, Laitner MH. Uterine Fibroids: Assessing Unmet Needs from Bench to Bedside. J Womens Health 2021; 30(8): 1060-1067.
5. Han J, Wang X, Lv W, Tian RY, Guan L. Comparison between direct use and PLGA nanocapsules containing drug of traditional Chinese medicine, Tiaojing Zhixue, in treatment of dysfunctional uterine bleeding. Cell Mol Biol 2021; 67(3): 138-142.
6. Coutinho LM, Assis WA, Spagnuolo-Souza A, Reis FM. Uterine Fibroids and Pregnancy: How Do They Affect Each Other? Reprod Sci 2022; 29(8): 2145-2151.
7. Stewart EA, Nowak RA. Uterine Fibroids: Hiding in Plain Sight. Physiology 2022; 37(1): 16-27.
8. Laughlin-Tommaso SK, Hesley GK, Hopkins MR, Brandt KR, Zhu Y, Stewart EA. Clinical limitations of the International Federation of Gynecology and Obstetrics (FIGO) classification of uterine fibroids. Int J Gynecol Obstet 2017; 139(2): 143-148.
9. Ciebiera M, Esfandyari S, Siblini H, et al. Nutrition in Gynecological Diseases: Current Perspectives. Nutrients 2021; 13(4):
10. Munro MG. Uterine polyps, adenomyosis, leiomyomas, and endometrial receptivity. Fertil Steril 2019; 111(4): 629-640.
11. Machado-Lopez A, Simon C, Mas A. Molecular and Cellular Insights into the Development of Uterine Fibroids. Int J Mol Sci 2021; 22(16):
12. Hadish JA, Biggs TD, Shealy BT, et al. GEMmaker: process massive RNA-seq datasets on heterogeneous computational infrastructure. Bmc Bioinformatics 2022; 23(1): 156.
13. Ren Z, Li W, Liu Q, Dong Y, Huang Y. Profiling of the Conjunctival Bacterial Microbiota Reveals the Feasibility of Utilizing a Microbiome-Based Machine Learning Model to Differentially Diagnose Microbial Keratitis and the Core Components of the Conjunctival Bacterial Interaction Network. Front Cell Infect Mi 2022; 12: 860370.
14. Li Z, Yin H, Chen K, et al. Effects of bisphenol A on uterine leiomyoma: In vitro and in vivo evaluation with mechanistic insights related to XBP1. Ecotox Environ Safe 2022; 247: 114201.
15. Carbajo-Garcia MC, Juarez-Barber E, Segura-Benitez M, et al. H3K4me3 mediates uterine leiomyoma pathogenesis via neuronal processes, synapsis components, proliferation, and Wnt/beta-catenin and TGF-beta pathways. Reprod Biol Endocrin 2023; 21(1): 9.
16. Carbajo-Garcia MC, de Miguel-Gomez L, Juarez-Barber E, et al. Deciphering the Role of Histone Modifications in Uterine Leiomyoma: Acetylation of H3K27 Regulates the Expression of Genes Involved in Proliferation, Cell Signaling, Cell Transport, Angiogenesis and Extracellular Matrix Formation. Biomedicines 2022; 10(6):
17. Moore LD, Le T, Fan G. DNA methylation and its basic function. Neuropsychopharmacol 2013; 38(1): 23-38.
18. Li Y, Ran R, Guan Y, Zhu X, Kang S. Aberrant Methylation of the E-Cadherin Gene Promoter Region in the Endometrium of Women With Uterine Fibroids. Reprod Sci 2016; 23(8): 1096-1102.
19. Bryan S, Zipp G, Breitkreuz D. The Effects of Mindfulness Meditation and Gentle Yoga on Spiritual Well-Being in Cancer Survivors: A Pilot Study. Altern Ther Health M 2021; 27(3): 32-38.
20. Vogelstein B, Papadopoulos N, Velculescu VE, Zhou S, Diaz LJ, Kinzler KW. Cancer genome landscapes. Science 2013; 339(6127): 1546-1558.
21. Joubert KS, George BP, Razlog R, Abrahamse H. A Review of Preclinical Research on the Effects of Photodynamic Therapy and Homeopathic Medicine on Cancer Cells. Altern Ther Health M 2021; 27(6): 40-50.
22. Joo JH, Oh H, Kim M, et al. NADPH Oxidase 1 Activity and ROS Generation Are Regulated by Grb2/Cbl-Mediated Proteasomal Degradation of NoxO1 in Colon Cancer Cells. Cancer Res 2016; 76(4): 855-865.
23. Oshima H, Ishikawa T, Yoshida GJ, et al. TNF-alpha/TNFR1 signaling promotes gastric tumorigenesis through induction of Noxo1 and Gna14 in tumor cells. Oncogene 2014; 33(29): 3820-3829.
24. Markowski DN, Helmke BM, Bartnitzke S, Loning T, Bullerdiek J. Uterine fibroids: do we deal with more than one disease? Int J Gynecol Pathol 2014; 33(6): 568-572.
25. Yang Q, Ciebiera M, Bariani MV, et al. Comprehensive Review of Uterine Fibroids: Developmental Origin, Pathogenesis, and Treatment. Endocr Rev 2022; 43(4): 678-719.
26. Salas A, Vazquez P, Bello AR, Baez D, Almeida TA. Dual agonist-antagonist effect of ulipristal acetate in human endometrium and

myometrium. Expert Rev Mol Diagn 2021; 21(8): 851-857.

27. Zierau O, Zenclussen AC, Jensen F. Role of female sex hormones, estradiol and progesterone, in mast cell behavior. Front Immunol 2012; 3: 169.

28. Jensen F, Woudwyk M, Teles A, et al. Estradiol and progesterone regulate the migration of mast cells from the periphery to the uterus and induce their maturation and degranulation. Plos One 2010; 5(12): e14409.

29. Lombardo J, Broadwater D, Collins R, Cebe K, Brady R, Harrison S. Hepatic mast cell concentration directly correlates to stage of fibrosis in NASH. Hum Pathol 2019; 86: 129-135.

30. Pilgrim J, Arismendi J, DeAngelis A, et al. Characterization of the role of Activator Protein 1 signaling pathway on extracellular matrix deposition in uterine leiomyoma. F S Sci 2020; 1(1): 78-89.

31. Biglia N, Carinelli S, Maiorana A, D'Alonzo M, Lo MG, Marci R. Ulipristal acetate: a novel pharmacological approach for the treatment of uterine fibroids. Drug Des Devel Ther 2014; 8: 285-292.

32. Mitchell JA, Shynlova O, Langille BL, Lye SJ. Mechanical stretch and progesterone differentially regulate activator protein-1 transcription factors in primary rat myometrial smooth muscle cells. Am J Physiol-Endoc M 2004; 287(3): E439-E445.